ACS ES&T Water

pubs.acs.org/estwater

Article

Unique Molecular Features of Water-Soluble Photo-Oxidation Products among Refined Fuels, Crude Oil, and Herded Burnt Residue under High Latitude Conditions

Elizabeth A. Whisenhant,* Phoebe Zito, David C. Podgorski, Amy M. McKenna, Zachary C. Redman, and Patrick L. Tomco

Cite This: *ACS EST Water* 2022, 2, 994–1002

Read Online

ACCESS | Metrics & More | Article Recommendations | Supporting Information

ABSTRACT: Photo-oxidized petroleum hydrocarbons are a unique class of water-soluble bioavailable compounds that have gained emerging recognition within toxic regulatory management bodies as an urgent and priority research need in high latitudes. In order to characterize the molecular signatures of photo-oxidized petroleum, bench-scale spills were irradiated over Alaskan seawater and freshwater at 5.5 °C. "Refined fuels" included heating oil, diesel, Jet-A, kerosene, and gasoline, with the Alaska North Slope (ANS) crude reference. An additional experiment assessed the photolytic aging of ANS crude "remediated" using a recently popularized strategy of *in situ* burning with and without herder application. A four-component fluorescence parallel factor model revealed a unique short-wavelength feature associated with photo-oxidized refined fuel that is not associated with traditional "microbial"- or "terrestrial-like" components. In contrast, crude oil photolytically decomposes into long-wavelength humic-like components (high humification index) and oxidized aliphatics. Fourier transform ion cyclotron resonance mass spectrometry data corroborated the optical data. Overall, on a per-volume basis, the refined fuels diesel, heating oil, kerosene, and Jet-A produce a significantly higher mass of photoproducts than crude oil and carry a unique chemical signature. This warrants new considerations regarding marine biota toxicity. This study also highlights new potential for tracking photo-modified water-soluble fractions of crude and refined fuels in high latitudes with fluorescence spectroscopy.

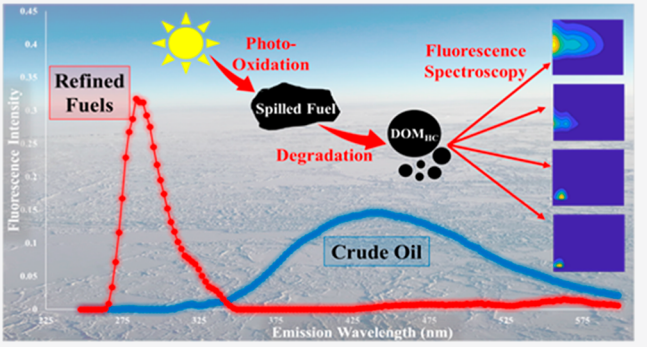

KEYWORDS: *dissolved organic matter, PARAFAC fluorescence, crude oil and diesel spill, FT-ICR MS, petroleum, photo-oxidation, photodegradation*

INTRODUCTION

As the Subarctic and Arctic continue to be a hub for oil exploration and production, methods of drilling, transportation, and product storage form a combination of efforts that enhance the risk of oil and fuel residuals entering the environment by large-scale spills and mechanical failures. Since tracking began in 1970, there have been over 57 000 spill incidents in Alaska reported by the Alaska Department of Environmental Conservation, with 12 000 of these reported incidents resulting from a structural or mechanical leak, line failure, or tank failure.[1] Spill incidents pose an increased risk in Alaska as spill detection is logistically difficult and expensive to access in remote regions. Additionally, the fate and transport of spilled chemicals in high-latitude regions are uniquely different from temperate environments due to sub-zero surface temperatures, short annual thaw season, and for terrestrial systems, restricted flow regimes from permafrost.[2] The ability to detect and fingerprint spilled fuel products and to develop spill response strategies in remote areas are imperative to locations susceptible to oil drilling and exploration as well as in areas that store aging fuel oil containers.

Petroleum introduced into the environment is subject to abiotic and biotic degradation processes. Photodegradation can oxidize petroleum to produce photoproducts by reacting with aromatic compounds that absorb light in the solar spectrum.[3−7] Microorganisms also produce oxygenated products through aerobic and anaerobic biodegradation processes.[8−11] Both photodegradation and biodegradation pathways can enhance the water solubility of petroleum products, resulting in the production of hydrocarbon-derived dissolved organic matter (DOM_{HC}), which encompasses the entire

Received: December 21, 2021
Revised: April 27, 2022
Accepted: April 28, 2022
Published: May 13, 2022

https://doi.org/10.1021/acsestwater.1c00494
ACS EST Water 2022, 2, 994–1002

continuum of parent and partially degraded compounds.[7,12−14] Once mobilized as a result of dissolution, DOM_{HC} can spread throughout the water column, potentially traveling undetected vast distances ahead of any signs of a visible oil front, increasing bioavailability, and impacting aquatic ecosystems both marine and freshwater. Photo-oxidized DOM_{HC} has received significant recent attention and has been identified as an urgent research priority to support oil spill response models.[15,16]

Several recent methods of petroleum fingerprinting have been described that characterize DOM_{HC} in aquatic systems.[17−21] DOM_{HC} contains chromophores that allow measurement and visualization through optical tools such as three-dimensional excitation-emission matrix spectroscopy (EEMs).[22] These approaches have been shown to be an effective method of detecting dispersed oil and chemically dispersed oil in open oceans, fingerprinting oil based on EEMs, and determining concentrations of benzene-toluene-ethylbenzene-xylene as well as total petroleum hydrocarbons and polycyclic aromatic hydrocarbons.[23−28] Fluorescence spectroscopy has also been applied to dissolved organic matter in arctic systems, largely in the context of labile and refractory pools.[28−30] DOM_{HC} is also commonly analyzed using modern Fourier transform ion cyclotron resonance mass spectrometry (FT-ICR MS).[6,7,20,31,32] These tools are complementary as parallel factor (PARAFAC) analysis can be used to deconvolute EEM spectra into individual components in an effort to identify chromophores present in DOM_{HC},[33,34] while FT-ICR MS can deconvolute complex petroleum spectra into molecular components aliphatic, aromatic, condensed aromatic (CA), and unsaturated high/low oxygenated species in van Krevelen space.[35,36] DOM_{HC}, treated as a unique complex mixture, has received recent attention in cold climates.[32] However, the photolytic decomposition of DOM_{HC} has not been classified in this regard, and to date, no information to our knowledge exists that assesses water-soluble photo-oxidized molecular features across a spectrum of fuel types and a gradient of irradiation times using these advanced techniques.

This study investigates the molecular properties of DOM_{HC} produced from films of crude oil and refined fuels (heating oil, diesel, Jet A, kerosene, and gasoline) that were subjected to simulated spill conditions of high latitudes. Additionally, this study assesses photo-modified dissolution of a popular crude oil spill remediation strategy, *in situ* burning following chemical herder application, which has gained recent popularity as a strategy for oil removal in cold regions.[37−40] This study aims to discover two main areas that are of urgent concern to stakeholders in the Arctic: (1) the extent of photo-modified solubility potential of each of these fuel types and (2) patterns in DOM_{HC} that can be used for early detection of spills in remote Arctic regions. We hypothesize that there is a positive relationship between dissolved organic carbon (DOC) concentration and irradiation period and that photo-oxidation will produce unique molecular signatures as evidence of added petroleum-derived DOM_{HC} to aquatic ecosystems. The ability to identify distinct optical signatures of the DOM_{HC} formed from each treatment may facilitate new methods to rapidly screen for leaked DOM_{HC} in remote areas of the Arctic that are susceptible to spills and are unable to be reached in a timely manner.

MATERIALS AND METHODS

Materials and Sample collection. Refined fuels were commercially obtained from throughout Southcentral Alaska in January 2020. Heating oil and diesel fuel were obtained in Anchorage, Alaska, by Shoreside Petroleum, Jet A-50 fuel was provided by International Aviation Services, and both kerosene and unleaded gasoline were sourced locally in Anchorage. Alaska North Slope (ANS) crude oil was obtained from the Valdez Marine Terminal in March 2018. Freshwater was collected from Otter Lake on Joint Base Elmendorf-Richardson, Alaska, and seawater was obtained from Resurrection Bay in Seward, Alaska, at the Alaska SeaLife Center. Water was filtered through pre-combusted (500 °C, >5 h) 0.27 μm glass microfiber filters (ADVANTEC) prior to the experiments. Glassware was acid-washed and combusted at 500 °C for 5 h.

Simulated Exposures. In the first experiment, films of fuel/crude oil were created at an oil load of 1.15 mL per 90 mL water in thermostatically controlled 100 mL jacketed beakers (Chemglass USA). Fuel types included heating oil, Jet A-50 fuel, unleaded gasoline, diesel fuel, kerosene, ANS crude oil, and burnt ANS crude oil. Each fuel treatment was applied over either freshwater or seawater (replicates of 3, total of 384 samples) and placed inside a solar simulator 12 samples at a time (Atlas Suntest XLS+, Atlas Material Testing Technology LLC). Solar irradiance was programmed at 250 W/m^2, equivalent to the daily summer maximum in Southcentral Alaska.[41] Each jacketed beaker was thermostatically controlled at 5.5 °C and represents a single time period from 0 to 240 h (0 to 10 days). Beakers were covered with quartz lids to allow for light transmittance and secured to reduce evaporation. After incubation, the samples were transferred to separatory funnels in order to isolate undissolved fuel from water. Water layers were filtered with 0.27 μm glass fiber filters. Samples were stored at 4 °C in the dark until analysis within 24 h or kept frozen until analyzed.

In the second experiment, crude oil (50 mL) was added to 4.5 L of seawater in 5 L high-density polyethylene jars secured with acrylic UV-transmitting covers. Two treatment types were tested: (1) *in situ*-burned (ISB) crude oil and (2) ISB crude oil after addition of a chemical herder (Siltech OP-40). In the first treatment group, crude oil was set aflame immediately after a thin film of oil covered the water. In the second treatment, the Siltech OP-40 chemical herder was added to the perimeter of the spilled oil film, and then burned. After burning, treatment groups underwent light regiments of UV exposure or complete darkness for 0 to 240 h (0 to 10 days). Each exposure chamber was controlled at 15 °C, the lowest achievable temperature for the given light intensity and experiment duration using a SunCool air conditioner. The remaining exposure and post-processing parameters followed procedures outlined in the first microcosm experiment.

DOC and EEM Measurements. DOC measurements were carried out using a Shimadzu TOC-L (Kyoto, Japan). Samples were acidified to pH 2 using 12 M HCl and sparged for 5 min with ultrapure air to eliminate volatiles and inorganic carbon. EEM spectra were collected using a HORIBA Aqualog Fluorometer (HORIBA Scientific, Kyoto, Japan). Further details of spectral acquisition, processing, and model validation are provided in the Supporting Information.

Ultrahigh-Resolution Mass Spectrometry. DOM_{HC} was isolated by a solid-phase extraction method and prepared for

https://doi.org/10.1021/acsestwater.1c00494
ACS EST Water 2022, 2, 994−1002

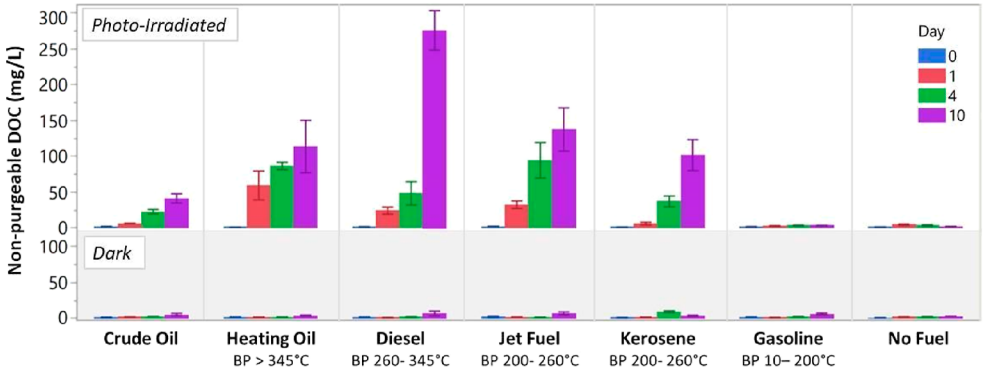

Figure 1. Temporal trends in non-purgeable DOC accumulation in water-soluble fractions following solar irradiation (top) and dark-incubated (bottom) among crude and refined fuels, with no-fuel control (natural water) (N = 6, ±1 SE). Petroleum types are listed in order of decreasing boiling point.[49]

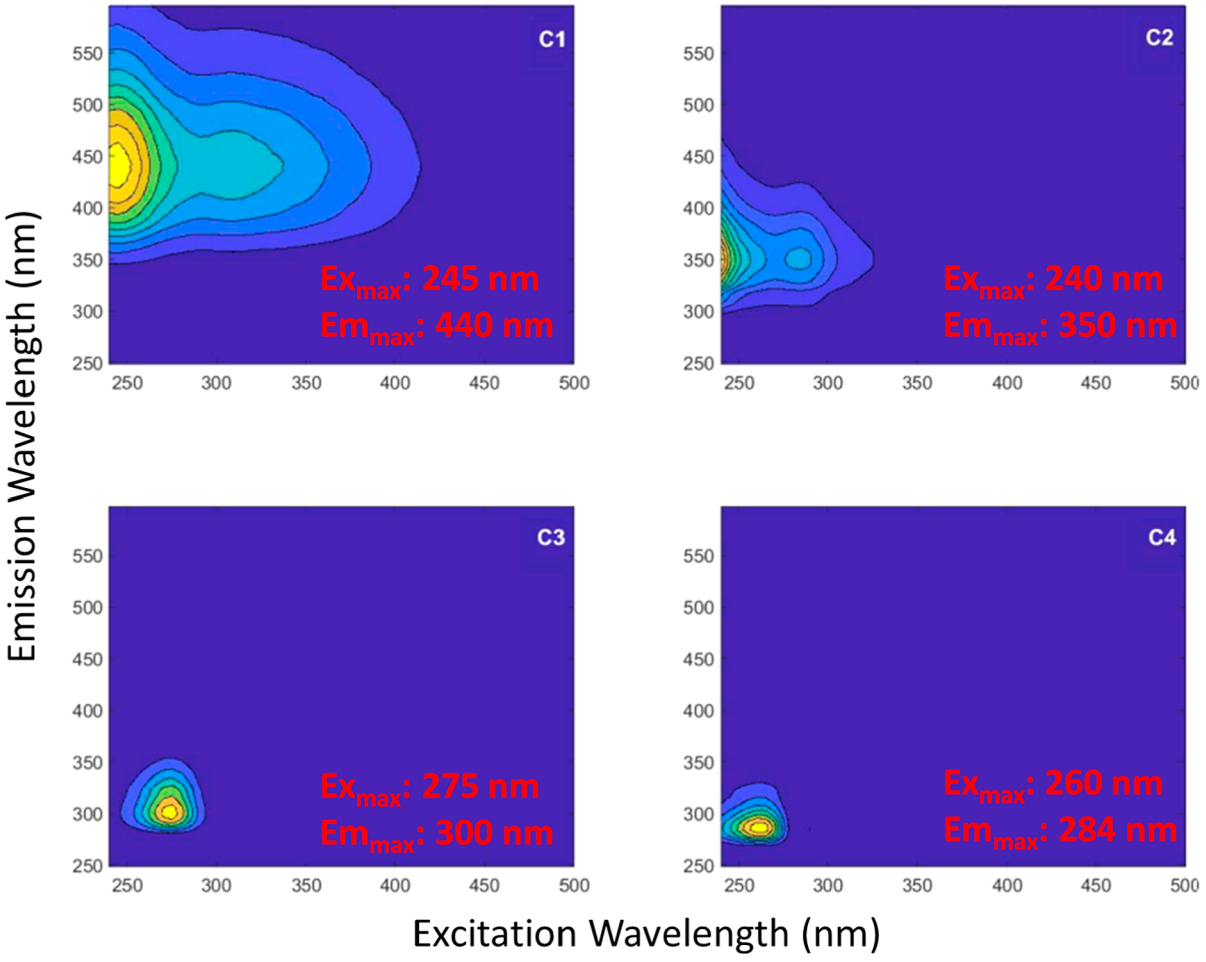

Figure 2. Two-dimensional contour plot of a four-component model validated by PARAFAC.

FT-ICR MS analysis. Aqueous samples were first acidified to pH 2 and passed through a Bond Elut PPL (Agilent Technologies) cartridge.[42] Acidified water (pH 2, Milli-Q water) was then passed through the cartridge to rinse any salts from the sample. DOM_{HC} selectively adsorbed onto the solid stationary phase, which was then dried using N_2 gas and eluted with 100% MeOH to a final concentration of 50 μg C mL^{-1}. DOM_{HC} extracts were infused by microelectrospray ionization at 500 mL min^{-1} and then analyzed using a hybrid linear ion trap FT-ICR mass spectrometer equipped with a 21 Tesla superconducting solenoid magnet.[43,44] ESI(−) is a common ionization source for determining oxidized petroleum products due to its ability to ionize acidic and polar compounds. Molecular formulas were assigned to signals with a magnitude greater than 6σ from the root mean squared baseline noise at m/z 500 using PetroOrg(c) software developed at the National High Magnetic Field Laboratory.[45] The reproducibility of FT-MS spectra for DOM analysis is reported in detail by Hawkes et al. 2020.[46] The molecular formulae were classified based on stoichiometry: CA (modified aromaticity index ($AI_{mod} \geq 0.67$), aromatic ($0.67 > AI_{mod} > 0.5$), unsaturated, low oxygen (ULO) ($AI_{mod} < 0.5$, H/C < 1.5, O/C < 0.5), unsaturated, high oxygen

https://doi.org/10.1021/acsestwater.1c00494
ACS EST Water 2022, 2, 994−1002

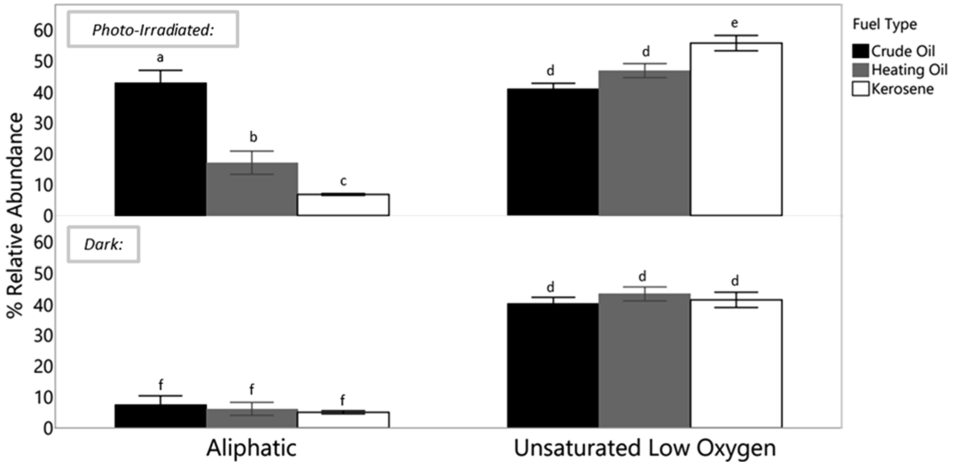

Figure 3. Aliphatic and ULO molecular characteristics of DOM_{HC} at 10 day irradiation time for crude oil, heating oil, and kerosene. Data are expressed as % relative abundance, $N = 4 \pm$ SE. Connecting letters for aliphatic (a,b,c,f) and ULO (d,e) are Student's *t*-test pairwise comparisons at 95% confidence.

(UHO) ($AI_{mod} < 0.5$, H/C < 1.5, O/C ≥ 0.5), aliphatic (H/C ≥ 1.5).[35,36,47]

RESULTS AND DISCUSSION

Dissolved Organic Carbon. Non-purgeable DOC concentrations in treatments exposed to sunlight increased with exposure time (Figure 1), while minimal change was observed in the treatments without light. DOC among all samples without light ranged from 0.79 ± 0.08 to 3.34 ± 2.95 mg/L at day 0 and ranged from 2.72 ± 0.30 to 10.58 ± 11.12 mg/L at day 10 (Table S3a–d). DOC among all samples after light treatment ranged from 0.80 ± 0.08 to 2.50 ± 0.95 mg/L at day 0 and 1.65 ± 0.56 to 323.67 ± 29.27 mg/L at day 10 (Table S3a–d). Concentrations of DOC at day 10 varied significantly by fuel type after light treatment but did not show a positive correlation between the boiling point of fuel and concentration of DOC present (Figure 1). Increases in DOC for refined fuels (kerosene, jet fuel, diesel, and heating oil) were greater compared to crude oil, consistent with what is known about the heavy components of crude oil requiring more extensive oxygenation before becoming water-soluble.[48] Gasoline did not exhibit an increase in DOC concentrations as the samples were sparged prior to analysis. DOC concentrations, along with other molecular features (discussed below), did not differ between freshwater and seawater conditions; for Figure 1, data were pooled for both water types ($N = 6$).

PARAFAC Analysis. PARAFAC highlights several changes in the DOM_{HC} composition over time. Figure 2 presents the four-component model validated for the DOM_{HC} samples. Component 1 (C1) exhibited excitation and emission (*Ex*/*Em*) maxima of 245/440 nm associated with signatures similar to terrestrial fulvic and humic-like substances (98% OpenFluor similarity score), suggesting that as petroleum is photodegraded, DOM_{HC} products resemble, among others, terrestrial materials (*i.e.*, high MW, oxidized, alicyclic/aromatic compounds).[30,50,51] The remaining components identify with common fluorophores with a 95% OpenFluor similarity score. Component 2 (C2, *Ex*/*Em*: 240/350 nm) resembles a tryptophan-like peak and is comparable to sources of seawater and freshwater streams.[34,52] Component 3 (C3, *Ex*/*Em*: 275/300 nm) represents a tyrosine-like peak comparable to terrestrial DOM offshore studies.[51,53] Component 4 (C4, *Ex*/*Em*: 260/284 nm) exhibited *Ex*/*Em* similar to one other component in the OpenFluor database, which matches the amino acid phenylalanine.[54] However, no phenylalanine was present in the samples when further examined (data not shown, see the Supporting Information). C4 is a new signature that is not indicative of a microbial-like (C2, C3) or terrestrial-like (C1) component, suggesting that there is a unique component revealing a petroleum fingerprint.

Humification index (HIX) values are determined by a ratio of long/short wavelength fluorescence. Typically, large HIX values are consistent with "humified", water-soluble, oxidized compounds.[55] An increase in HIX is an indication of a relative increase in long-wavelength DOM and/or depletion of short-wavelength DOM. HIX changes were noted across the incubation period for light-exposed treatments versus dark controls (Table S3a–d). Among irradiated samples, there is a consistent HIX increase for crude oil (Table S3d). For heating oil and jet fuel, HIX increased from 0 to 4 days, while no increase was noted for gasoline, diesel, or kerosene. This trend is consistent with the compounds that are expected to be present within the reported boiling points of each fuel type. Among the fuels we tested ($N = 6$ and 4 for EEMs and FT-ICR MS, respectively), DOM_{HC} produced from crude oil exhibited the most consistent increase in humification. This result is due to the broad range of molecular structures that are present in a whole crude, including those with high boiling points.[7] Conversely, gasoline revealed no increase in humification because it consists of a narrow range of carbon numbers from C4 to C12. However, among DOC measurements (Figure 1), we observed a greater extent of photo-modified DOC production from fuel types that are lighter than crude oil. This result indicates that the compounds that comprise these relatively (to whole crude oil) narrow carbon number range distillation cuts are susceptible to photo-oxidation. This point can be visualized by double-bond equivalent versus carbon number plots (Figure S3) and nominal oxidation states of carbon (NOSC, Figure S4). Moreover, the concentration of DOC produced from the refined fuels was an indication of the higher per-volume proportion of compounds in a distillate cut that can partition into the aqueous phase after a given period of photo-oxidation. This process provides a plausible explanation for the high DOC concentrations produced after 10 days of exposure from the diesel relative to the heating oil.

https://doi.org/10.1021/acsestwater.1c00494
ACS EST Water 2022, 2, 994–1002

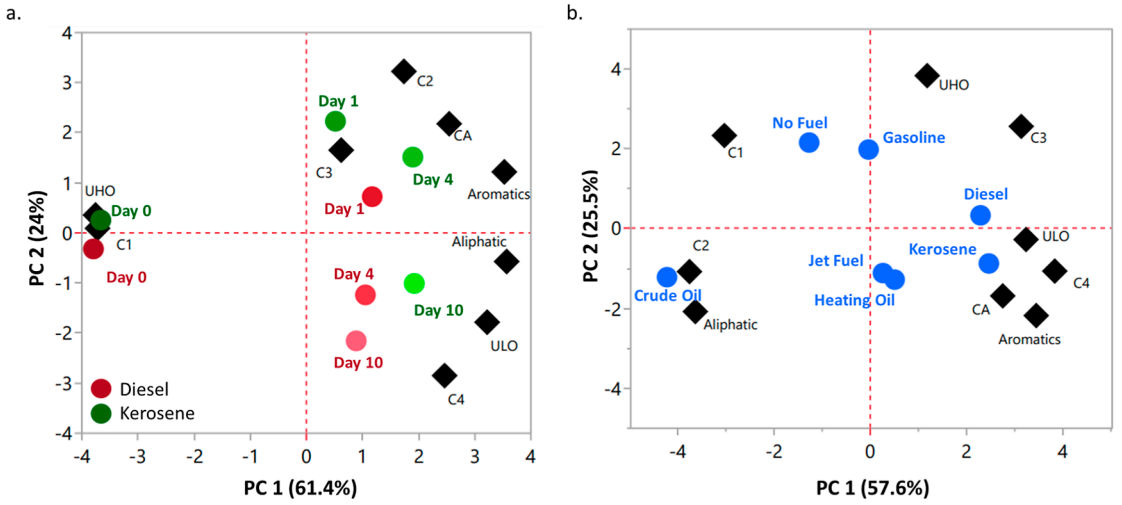

Figure 4. PCA biplots; loadings represent molecular features (fluorescence components C1−C4 and FT-ICR MS van Krevelen Space). (a) Compositional trends illustrated across time (irradiation period) from 0 to 10 days for two representative refined fuels, diesel and kerosene. These fuels exhibited similar trends compared to most other distillate cuts. (b) Molecular features present at an irradiation period = 10 days, the end irradiation time, and where maximum photo-product formation had occurred.

It is expected that an increase in the exposure period would result in an increase in DOC production from the fuel oil, which would eventually exceed that of diesel fuel. This result would be consistent with a DOC production continuum model that was previously reported on two crude oils with different chemical compositions.[7] Nevertheless, the compounds in the refined fuels are photolabile and more susceptible to photolysis, yet the product of degradation (DOM_{HC}) does not appear to be humic-like. Further study is needed to test the optical variances among products of different refining techniques to understand how these processes react photochemically.

Temporal Molecular Characteristics of DOM_{HC} following Irradiation. Ultrahigh-resolution mass enables a closer examination of the chemical composition of the polar DOM_{HC} products derived from each fuel type at the molecular level.[56] The percent relative abundances of the formulae classifications for each treatment are reported in Table S6a,b. In summary, the results obtained by mass spectrometry indicate that the chemical composition of photosolubilized DOM_{HC} is dependent on the composition of the initial distillate. This result corroborates previous reports showing that the composition of DOM_{HC} from whole crude oils is dependent on the initial composition of the crude.[7] To emphasize oxidation trends among the entire range of distillate cuts, Figure 3 highlights compositional differences in the aliphatic and ULO classes of DOM_{HC} produced from kerosene, crude oil, and heating oil after 10 days of light exposure and a dark control.

Crude oil produced the highest relative abundance of aliphatic DOM_{HC} (43.0 ± 4.0%). The DOM_{HC} produced from the heating oil, which has the highest boiling point of the distillates that we analyzed, has the second most abundant class of aliphatics (17.1 ± 3.8%). The abundance of aliphatics in the DOM_{HC} from kerosene, the second lowest boiling distillate cut, was the least (6.8 ± 0.3%) relative to that of crude oil and heating oil. On the other hand, trends in ULO relative abundances were inversely correlated to aliphatics for these fuels (Figure 3), with crude oil, heating oil, and kerosene at 41.0 ± 1.9, 46.9 ± 2.3, and 55.8 ± 2.5%, respectively. These data indicate that a relationship exists between the distillate fraction boiling point and the abundance of water-soluble photoproducts. van Krevelen subtraction plots for endmember timepoints T0, T10, and T10-0 further illustrate the compositional patterns for each fuel type in seawater and freshwater (Figures S5 and S6).

When compared to dark controls, aliphatic-like DOM_{HC} was produced by photo-irradiating crude oil, heating oil, and kerosene. This is consistent with previous studies that investigated other photo-oxidized crude oils and weathered tarballs, where similarly, water-soluble aliphatic production was noted following exposure to simulated sunlight.[6,7,48,57] ULO relative abundances increased only for kerosene (Figure 3). This suggests that distillate cuts at lower boiling points will form photoproducts with higher relative abundances of ULO and lower relative abundances of aliphatics. NOSC was, in general, lower for irradiated samples versus dark controls (Figure S4). Interestingly however, the NOSC data indicate temporal variations among fuel types. Jet fuel and heating oil exhibited minimum NOSC with 1 day irradiation, while NOSC decreased with irradiation time throughout 10 days. These trends note the unique temporal and fuel type dependency on photoproduct formation.

Principal component analysis (PCA) further supports the uniqueness of component C4; as refined fuel samples experienced photo-irradiation, fuel-derived DOM_{HC} fluorophores were formed with an increased relative abundance of molecular signatures representative of C4 (Figure 4A). This trend is consistent for most refined fuels (Figure 4B) as the PCA of all fuel types at 10 day exposure demonstrates that DOM_{HC} produced from diesel, kerosene, Jet-A, and heating oil clustered with loadings for C4, which itself clustered with the loadings for ULO, aromatic, and CA. It is important to note that these groupings represent ESI(−) ionizable compounds, which are polar in nature and the operational definition of CA, aromatics, and aliphatics are not bracketed by O/C; therefore, the features observed represent polar, oxidized forms. Crude oil is unique from these other fuel types, closely resembling C2 and aliphatic (oxidized aliphatic) over time. The temporal trends toward C4 did not differ between freshwater and seawater (Figures S1 and S2). We found C4 to be a unique

https://doi.org/10.1021/acsestwater.1c00494
ACS EST Water 2022, 2, 994−1002

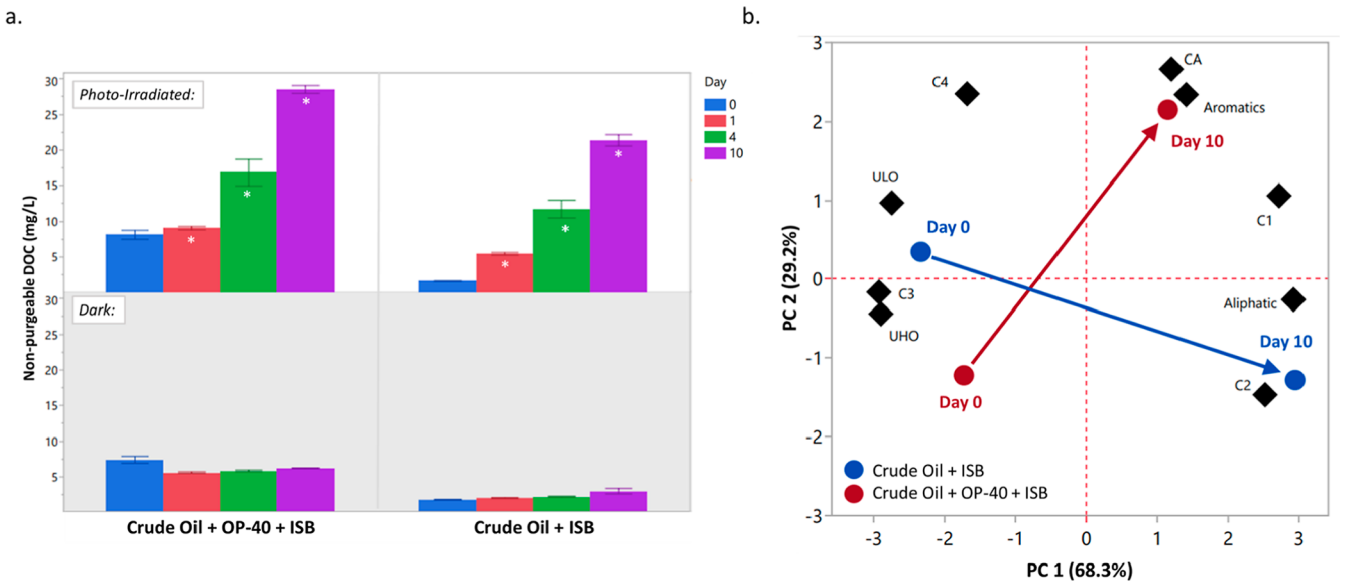

Figure 5. DOC and PCA plots of ISB crude oil treatments. (a) Non-purgeable DOC under light and dark conditions (N = 3, ±1 SE). Significance (*) between light and dark conditions for the same time point is denoted by pairwise comparisons (Student's t-test, 95% confidence). (b) PCA of photo-irradiated ISB and OP40 + ISB samples over time, days 0 and 10.

fluorescent component accompanying the photo-production of DOM_{HC} from diesel and kerosene and, to a lesser extent, jet fuel and heating oil.

Photo-Modified Solubility of Burned versus Herded Burned Crude Oil. Following exposure to simulated sunlight, DOC concentrations for both ISB and OP40 (herder)+ISB increased relative to samples under total darkness (Figure 5A). Samples that were irradiated for 10 days yielded DOC concentrations that were 13.3 and 3.5 times higher than those of day 0 for oil + ISB and oil + OP40 + ISB, respectively (Table S8). Absence of photo-irradiation and DOC concentrations for oil + OP40 + ISB and oil + ISB at day 10 were 1.2 times lower and 1.7 times higher, respectively, than at day 0. Furthermore, the overall DOC concentrations in oil + OP40 + ISB were higher than that of oil + ISB (Figure 5A). This result indicates strongly that herder addition increases DOC relative to non-herded burned oil and that herded burnt residues are capable of producing more photo-products that have more oxidized aromatic and oxidized CA character (Figure 5B). These results are consistent with known pathways of formation, dissolution, and reactivity of other classes of pyrogenic black carbon substrates in aquatic ecosystems.[58−61] PCA plots revealed that samples at day 0 are dominated by C3 (tyrosine-like), and over 10 day sunlight exposure, they modulate toward C1 (humic-like) (Figure 5B). Still, DOM_{HC} produced from each crude oil treatment yields terrestrial-like chromophoric products under sunlight exposure, and there is a consistent HIX increase for both crude oil treatment groups among irradiated samples (Table S8). Future research is needed to better classify specific byproducts and their corresponding toxicity.[62−69]

CONCLUSIONS

This study presents preliminary, but important data comparing the photo-modification effects of spilled petroleum on solubility, which is a significant factor that accompanies weathering. We describe the temporal trends in molecular features among several common fuel types, primarily indicating an increased production of oxidized aliphatics and aromatics. Increased DOC concentrations were observed in all spilled samples after light treatment relative to no fuel, with the exception of gasoline, which did not weather into a non-purgeable form of DOM_{HC}. Most notable is the uniqueness of photo-products between crude oil and refined fuels. PARAFAC and FT-ICR MS analysis highlighted the continuum where spilled fuels and crude oil were oxidized into DOM_{HC} and were discernible by specific fluorescence components and molecular features. All crude oil samples, including burnt and herded burnt residues, exhibited humic-like fluorescence wavelengths, while refined fuels exhibited an undefined component discernible from crude oil-derived and protein-derived components. PCA and HIX demonstrated that DOM_{HC} from refined fractions may not weather into humic-like components but rather C4-like, oxidized aromatics, and oxidized CAs. This difference sets an encouraging precedent for fuel photo-oxidation studies and detection protocols of these compounds in cold climates.

ASSOCIATED CONTENT

Supporting Information

The Supporting Information is available free of charge at https://pubs.acs.org/doi/10.1021/acsestwater.1c00494.

Experimental design; experimental methods; analytical test for phenylalanine; experimental design; ISB experimental design; DOC concentrations, SUVA254, and spectral index of refined fuel versus the crude oil experiment; fluorescence component contributions of refined fuels and crude oil experiments; fluorescent component matches to studies on the OpenFluor database; PCA plot of fluorescence components between freshwater and seawater; FT-ICR MS molecular classifications per fuel type; FT-ICR MS molecular classifications of oil + ISB and oil + ISB + OP40; PCA plot of FT-ICR MS molecular classifications between freshwater and seawater; double bond equivalent versus carbon number plots of freshwater and seawater samples

https://doi.org/10.1021/acsestwater.1c00494
ACS EST Water 2022, 2, 994−1002

at 10 days of light exposure and dark controls; NOSC plot of fuel types at 0−10 days of light exposure and dark controls; van Krevelen plots of refined fuels and crude oil in freshwater; van Krevelen plots of refined fuels and crude oil in seawater; DOC concentrations, SUVA254, and spectral index of the oil + ISB and oil + ISB + OP40 experiment; and fluorescence component contributions of the oil + ISB and oil + ISB + OP40 experiment (PDF)

AUTHOR INFORMATION

Corresponding Author

Elizabeth A. Whisenhant − *Department of Chemistry, University of Alaska Anchorage, Anchorage, Alaska 99508, United States; Department of Chemistry, Chemical Analysis & Mass Spectrometry Facility, University of New Orleans, New Orleans, Louisiana 70148, United States;* orcid.org/0000-0001-5167-6797; Phone: 907-786-1260; Email: eawhisen@uno.edu

Authors

Phoebe Zito − *Department of Chemistry, University of Alaska Anchorage, Anchorage, Alaska 99508, United States; Department of Chemistry, Chemical Analysis & Mass Spectrometry Facility, University of New Orleans, New Orleans, Louisiana 70148, United States*

David C. Podgorski − *Department of Chemistry, University of Alaska Anchorage, Anchorage, Alaska 99508, United States; Department of Chemistry, Chemical Analysis & Mass Spectrometry Facility, University of New Orleans, New Orleans, Louisiana 70148, United States; Pontchartrain Institute for Environmental Sciences, Shea Penland Coastal Education and Research Facility, University of New Orleans, New Orleans, Louisiana 70148, United States;* orcid.org/0000-0002-1070-5923

Amy M. McKenna − *National High Magnetic Field Laboratory, Florida State University, Tallahassee, Florida 32310, United States; Department of Soil and Crop Sciences, Colorado State University, Fort Collins, Colorado 80523, United States;* orcid.org/0000-0001-7213-521X

Zachary C. Redman − *Department of Chemistry, University of Alaska Anchorage, Anchorage, Alaska 99508, United States;* orcid.org/0000-0002-4158-524X

Patrick L. Tomco − *Department of Chemistry, University of Alaska Anchorage, Anchorage, Alaska 99508, United States*

Complete contact information is available at: https://pubs.acs.org/10.1021/acsestwater.1c00494

Funding

Funding from this project was provided by the UAA ConocoPhillips Arctic Science and Engineering Endowment and NSF #1929173 to P.L.T.

Notes

The authors declare no competing financial interest.

ACKNOWLEDGMENTS

Funding for this project was provided by the UAA ConocoPhillips Arctic Science and Engineering Endowment and NSF #1929173 to P.L.T. A portion of this work was performed at the National High Magnetic Field Laboratory ICR User Facility, which is supported by the National Science Foundation Division of Chemistry through DMR-1644779 and the State of Florida.

REFERENCES

(1) Alaska Department of Environmental Conservation, PPR Spills Database Search. https://dec.alaska.gov/Applications/SPAR/PublicMVC/PERP/SpillSearch (accessed Dec 13, 2021).

(2) Wagner, A. M.; Barker, A. J. Distribution of polycyclic aromatic hydrocarbons (PAHs) from legacy spills at an Alaskan Arctic site underlain by permafrost. *Cold Reg. Sci. Technol.* **2019**, *158*, 154−165.

(3) Ray, P. Z.; Tarr, M. A. Solar Production of Singlet Oxygen from Crude Oil Films on Water. *J. Photochem. Photobiol., A* **2014**, *286*, 22−28.

(4) Ray, P. Z.; Tarr, M. A. Petroleum films exposed to sunlight produce hydroxyl radical. *Chemosphere* **2014**, *103*, 220−227.

(5) Ray, P. Z.; Tarr, M. A. Formation of organic triplets from solar irradiation of petroleum. *Mar. Chem.* **2015**, *168*, 135−139.

(6) Ray, P. Z.; Chen, H.; Podgorski, D. C.; McKenna, A. M.; Tarr, M. A. Sunlight creates oxygenated species in water-soluble fractions of Deepwater horizon oil. *J. Hazard. Mater.* **2014**, *280*, 636−643.

(7) Zito, P.; Podgorski, D. C.; Johnson, J.; Chen, H.; Rodgers, R. P.; Guillemette, F.; Kellerman, A. M.; Spencer, R. G. M.; Tarr, M. A. Molecular-level composition and acute toxicity of photosolubilized petrogenic carbon. *Environ. Sci. Technol.* **2019**, *53*, 8235−8243.

(8) Hazen, T. C.; Prince, R. C.; Mahmoudi, N. Marine oil biodegradation. *Environ. Sci. Technol.* **2016**, *50*, 2121−2129.

(9) Townsend, G. T.; Prince, R. C.; Suflita, J. M. Anaerobic oxidation of crude oil hydrocarbons by the resident microorganisms of a contaminated anoxic aquifer. *Environ. Sci. Technol.* **2003**, *37*, 5213−5218.

(10) Amos, R. T.; Bekins, B. A.; Cozzarelli, I. M.; Voytek, M. A.; Kirshtein, J. D.; Jones, E. J. P.; Blowes, D. W. Evidence for iron-mediated anaerobic methane oxidation in a crude oil-contaminated aquifer. *Geobiology* **2012**, *10*, 506−517.

(11) Fingas, M. *Analysis of Oil Biodegradation Products*; Prince William Sound Regional Citizens' Advisory Council, 2014.

(12) Podgorski, D.C.; Zito, P.; Kellerman, A.M.; Bekins, B.A.; Cozzarelli, I.M.; Smith, D.F.; Cao, X.; Schmidt-Rohr, K.; Wagner, S.; Stubbins, A.; Spencer, R.G.M. Hydrocarbons to carboxyl-rich alicylic molecules: A continuum model to describe biodegradation of petroleum-derived dissolved organic matter in contaminated groundwater plumes. *J. Hazard. Mater.* **2021**, *402*, 123998.

(13) Essaid, H. I.; Bekins, B. A.; Herkelrath, W. N.; Delin, G. N. Crude oil at the Bemidji site: 25 years of monitoring, modeling, and understanding. *Groundwater* **2011**, *49*, 706−726.

(14) Bekins, B. A.; Cozzarelli, I. M.; Erickson, M. L.; Steenson, R. A.; Thorn, K. A. Crude oil metabolites in groundwater at two spill sites. *Groundwater* **2016**, *54*, 681−691.

(15) Ward, C. P.; Sharpless, C. M.; Valentine, D. L.; French-McCay, D. P.; Aeppli, C.; White, H. K.; Rodgers, R. P.; Gosselin, K. M.; Nelson, R. K.; Reddy, C. M. Partial photochemical oxidation was a dominant fate of Deepwater Horizon surface oil. *Environ. Sci. Technol.* **2018**, *52*, 1797−1805.

(16) Barker, C. H.; Kourafalou, V. H.; Beegle-Krause, C.; Boufadel, M.; Bourassa, M. A.; Buschang, S. G.; Androulidakis, Y.; Chassignet, E. P.; Dagestad, K.-F.; Danmeier, D. G.; Dissanayake, A. L.; Galt, J. A.; Jacobs, G.; Marcotte, G.; Özgökmen, T.; Pinardi, N.; Schiller, R. V.; Socolofsky, S. A.; Thrift-Viveros, D.; Zelenke, B.; Zhang, A.; Zheng, Y. Progress in operational modeling in support of oil spill response. *J. Mar. Sci. Eng.* **2020**, *8*, 668.

(17) Bianchi, T. S.; Osburn, C.; Shields, M. R.; Yvon-Lewis, S.; Young, J.; Guo, L.; Zhou, Z. Deepwater Horizon oil in Gulf of Mexico waters after 2 years: transformation into the dissolved organic matter pool. *Environ. Sci. Technol.* **2014**, *48*, 9288.

(18) Zhou, Z.; Guo, L.; Shiller, A. M.; Lohrenz, S. E.; Asper, V. L.; Osburn, C. L. Characterization of oil components from the Deepwater Horizon oil spill in the Gulf of Mexico using fluorescence EEM and PARAFAC techniques. *Mar. Chem.* **2013**, *148*, 10−21.

(19) Murphy, K. R.; Boehme, J. R.; Brown, C.; Noble, M.; Smith, G.; Sparks, D.; Ruiz, G. M. Exploring the limits of dissolved organic matter fluorescence for determining seawater sources and ballast water exchange on the US Pacific coast. *J. Mar. Syst.* **2013**, *111*−*112*, 157−166.
(20) Dvorski, S. E.-M.; Gonsior, M.; Hertkorn, N.; Uhl, J.; Müller, H.; Griebler, C.; Schmitt-Kopplin, P. Geochemistry of dissolved organic matter in a spatially highly resolved groundwater petroleum hydrocarbon plume cross-section. *Environ. Sci. Technol.* **2016**, *50*, 5536−5546.
(21) Mirnaghi, F. S.; Pinchin, N. P.; Yang, Z.; Hollebone, B. P.; Lambert, P.; Brown, C. E. Monitoring of polycyclic aromatic hydrocarbon contamination at four oil spill sites using fluorescence spectroscopy coupled with parallel factor-principal component analysis. *Environ. Sci.: Processes Impacts* **2019**, *21*, 413−426.
(22) Murphy, K. R.; Stedmon, C. A.; Graeber, D.; Bro, R. Fluorescence spectroscopy and multi way techniques. *PARAFAC. Anal. Meth.* **2013**, *5*, 6557−6566.
(23) Keizer, P. D.; Gordon, D. C., Jr. Detection of trace amounts of oil in sea water by fluorescence spectroscopy. *J. Fish. Res. Board Can.* **1973**, *30*, 1039−1046.
(24) Bugden, J. B. C.; Yeung, C. W.; Kepkay, P. E.; Lee, K. Application of ultraviolet fluorometry and excitation-emission matrix spectroscopy (EEMS) to fingerprint oil and chemically dispersed oil in seawater. *Mar. Pollut. Bull.* **2008**, *56*, 677−685.
(25) Brown, C. E.; Fingas, M. F. Review of the development of laser fluorosensors for oil spill application. *Mar. Pollut. Bull.* **2003**, *47*, 477−484.
(26) Fingas, M.; Brown, C. Review of oil spill remote sensing. *Mar. Pollut. Bull.* **2014**, *83*, 9−23.
(27) Conmy, R. N.; Coble, P. G.; Farr, J.; Wood, A. M.; Lee, K.; Pegau, W. S.; Walsh, I. D.; Koch, C. R.; Abercrombie, M. I.; Miles, M. S.; Lewis, M. R.; Ryan, S. A.; Robinson, B. J.; King, T. L.; Kelble, C. R.; Lacoste, J. Submersible optical sensors exposed to chemically dispersed crude oil: wave tank simulations for improved oil spill monitoring. *Environ. Sci. Technol.* **2014**, *48*, 1803−1810.
(28) Driskill, A. K.; Alvey, J.; Dotson, A. D.; Tomco, P. L. Monitoring polycyclic aromatic hydrocarbon (PAH) attenuation in Arctic waters using fluorescence spectroscopy. *Cold Reg. Sci. Technol.* **2018**, *145*, 76−85.
(29) Chen, M.; Nam, S.-I.; Kim, J.-H.; Kwon, Y.-J.; Hong, S.; Jung, J.; Shin, K.-H.; Hur, J. High abundance of protein-like fluorescence in the Amerasian Basin of Arctic Ocean: Potential implication of a fall phytoplankton bloom. *Sci. Total Environ.* **2017**, *599*−*600*, 355−363.
(30) Hill, V. J.; Zimmerman, R. C. Characteristics of colored dissolved organic material in first year landfast sea ice and the underlying water column in the Canadian arctic in the early spring. *Mar. Chem.* **2016**, *180*, 1−13.
(31) Jaggi, A.; Radović, J. R.; Snowdon, L. R.; Larter, S. R.; Oldenburg, T. B. P. Composition of the Dissolved Organic Matter Produced During In Situ burning of Spilled. *Oil. Org. Geochem.* **2019**, *138*, 103926.
(32) Tomco, P. L.; Duddleston, K. N.; Driskill, A.; Hatton, J. J.; Grond, K.; Wrenn, T.; Tarr, M. A.; Podgorski, D. C.; Zito, P. Dissolved organic matter production from herder application and in-situ burning of crude oil at high latitudes: Bioavailable molecular composition patterns and microbial community diversity effects. *J. Hazard. Mater.* **2022**, *424*, 127598.
(33) Stedmon, C. A.; Markager, S.; Bro, R. Tracing dissolved organic matter in aquatic environments using a new approach to fluorescence spectroscopy. *Mar. Chem.* **2003**, *82*, 239−254.
(34) Murphy, K. R.; Stedmon, C. A.; Waite, T. D.; Ruiz, G. M. Distinguishing between terrestrial and autochthonous organic matter sources in marine environments using fluorescence spectroscopy. *Mar. Chem.* **2008**, *108*, 40−58.
(35) Koch, B. P.; Dittmar, T. From Mass to Structure: An Aromaticity Index for High-Resolution Mass Data of Natural Organic Matter. *Rapid Commun. Mass Spectrom.* **2006**, *20*, 926−932.
(36) Šantl-Temkiv, T.; Finster, K.; Dittmar, T.; Hansen, B. M.; Thyrhaug, R.; Nielsen, N. W.; Karlson, U. G. Hailstones: A Window into the Microbial and Chemical Inventory of a Storm Cloud. *PLoS One* **2013**, *8*, No. e53550.
(37) Bullock, R. J.; Perkins, R. A.; Aggarwal, S. In-situ burning with chemical herders for Arctic oil spill response: Meta-analysis and review. *Sci. Total Environ.* **2019**, *675*, 705−716.
(38) Aggarwal, S.; Schnabel, W.; Buist, I.; Garron, J.; Bullock, R.; Perkins, R.; Potter, S.; Cooper, D. Aerial application of herding agents to advance in-situ burning for oil spill response in the Arctic: A pilot study. *Cold Reg. Sci. Technol.* **2017**, *135*, 97−104.
(39) Buist, I.; Potter, S.; Nedwed, T.; Mullin, J. Herding surfactants to contract and thicken oil spills in pack ice for in situ burning. *Cold Reg. Sci. Technol.* **2011**, *67*, 3−23.
(40) Buist, I.; Cooper, D.; Trudel, K.; Fritt-Rasmussen, J.; Wegeberg, S.; Gustavson, K.; Lassen, P.; Jomaas, G.; Zabilansky, L. Research investigations into herder fate, effects and windows-of-opportunity. *Draft Report to Arctic Oil Spill Response Technology Joint Industry Programme (JIP)*, 2016; pp 1−156.
(41) Dissing, D.; Wendler, G. Solar radiation climatology of Alaska. *Theor. Appl. Climatol.* **1998**, *61*, 161−175.
(42) Dittmar, T.; Koch, B.; Hertkorn, N.; Kattner, G. A Simple and Efficient Method for the Solid-Phase Extraction of Dissolved Organic Matter (SPE-DOM) from Seawater. *Limnol. Oceanogr.: Methods* **2008**, *6*, 230−235.
(43) Smith, D. F.; Podgorski, D. C.; Rodgers, R. P.; Blakney, G. T.; Hendrickson, C. L. 21 Tesla FT-ICR Mass Spectrometer for Ultrahigh-Resolution Analysis of Complex Organic Mixtures. *Anal. Chem.* **2018**, *90*, 2041−2047.
(44) Hendrickson, C. L.; Quinn, J. P.; Kaiser, N. K.; Smith, D. F.; Blakney, G. T.; Chen, T.; Marshall, A. G.; Weisbrod, C. R.; Beu, S. C. 21 Tesla Fourier Transform Ion Cyclotron Resonance Mass Spectrometer: A National Resource for Ultrahigh Resolution Mass Analysis. *J. Am. Soc. Mass Spectrom.* **2015**, *26*, 1626−1632.
(45) Corilo, Y. E. *PetroOrg Software*; Florida State University, Omics LLC: Tallahassee, Fl, 2014.
(46) Hawkes, J. A.; D'Andrilli, J.; Sleighter, R. L.; Chen, H.; Hatcher, P. G.; Ijaz, A.; Khaksan, M.; Schum, S.; Mazzoleni, L.; Chu, R.; Tolic, N.; Kew, W.; Hess, N.; Lv, J.; Zhang, S.; Chen, H.; Shi, Q.; Hutchins, R. H. S.; Lozano, D. C. P.; Gavard, R.; Jones, H. E.; Thomas, M. J.; Barrow, M.; Osterholz, H.; Dittmar, T.; Simon, C.; Gleixner, G.; Berg, S. M.; Remucal, C. K.; Catalán, N.; Cole, R. B.; Noreiga-Ortega, B.; Singer, G.; Radoman, N.; Schmitt, N. D.; Stubbins, A.; Agar, J. N.; Zito, P.; Podgorski, D. C. An International Laboratory Comparison of Dissolved Organic Matter Composition by High Resolution Mass Spectrometry: Are We Getting the Same Answer? *Limnol. Oceanogr.: Methods* **2020**, *18*, 235−258.
(47) O'Donnell, J. A.; Aiken, G. R.; Butler, K. D.; Guillemette, F.; Podgorski, D. C.; Spencer, R. G. M. DOM Composition and Transformation in Boreal Forest Soils: The Effects of Temperature and Organic-Horizon Decomposition State. *J. Geophys. Res.: Biogeosci.* **2016**, *121*, 2727−2744.
(48) Zito, P.; Podgorski, D. C.; Bartges, T.; Guillemette, F.; Roebuck, J. A.; Spencer, R. G. M.; Rodgers, R. P.; Tarr, M. A. Sunlight induced molecular progression of oil into oxidized oil soluble species, interfacial material, and dissolved organic matter. *Energy Fuels* **2020**, *34*, 4721−4726.
(49) Aitani, A. Crude Oil Refining: Chemical Conversion. *Petrol. Econ. Eng.* **2013**, *3*, 325−344.
(50) Retelletti Brogi, S.; Ha, S.-Y.; Kim, K.; Derrien, M.; Lee, Y. K.; Hur, J. Optical and molecular characterization of dissolved organic matter (DOM) in the arctic ice core and the underlying seawater (Cambridge Bay, Canada): Implication for increased autochthonous DOM during ice melting. *Sci. Total Environ.* **2018**, *627*, 802−811.
(51) Painter, S. C.; Lapworth, D. J.; Woodward, E. M. S.; Kroeger, S.; Evans, C. D.; Mayor, D. J.; Sanders, R. J. Terrestrial dissolved organic matter distribution in the north sea. *Sci. Total Environ.* **2018**, *630*, 630−647.

https://doi.org/10.1021/acsestwater.1c00494
ACS EST Water 2022, 2, 994−1002

(52) Yamashita, Y.; Kloeppel, B. D.; Knoepp, J.; Zausen, G. L.; Jaffé, R. Effects of watershed history on dissolved organic matter characteristics in headwater streams. *Ecosystems* **2011**, *14*, 1110−1122.
(53) Yamashita, Y.; Boyer, J. N.; Jaffé, R. Evaluating the distribution of terrestrial dissolved organic matter in a complex coastal ecosystem using fluorescence spectroscopy. *Cont. Shelf Res.* **2013**, *66*, 136−144.
(54) D'Andrilli, J.; McConnell, J. R. Polar ice core organic matter signatures reveal past atmospheric carbon composition and spatial trends across ancient and modern timescales. *J. Glaciol.* **2021**, *67*, 1028−1042.
(55) Ohno, T.; Chorover, J.; Omoike, A.; Hunt, J. Molecular weight and humification index as predictors of adsorption for plant- and manure-derived dissolved organic matter to goethite. *Eur. J. Soil Sci.* **2007**, *58*, 125−132.
(56) McKenna, A. M.; Nelson, R. K.; Reddy, C. M.; Savory, J. J.; Kaiser, N. K.; Fitzsimmons, J. E.; Marshall, A. G.; Rodgers, R. P. Expansion of the Analytical Window for Oil Spill Characterization by Ultrahigh Resolution Mass Spectrometry: Beyond Gas Chromatography. *Environ. Sci. Technol.* **2013**, *47*, 7530−7539.
(57) Harriman, B. H.; Zito, P.; Podgorski, D. C.; Tarr, M. A.; Suflita, J. M. Impact of Photooxidation and Biodegradation on the Fate of Oil Spilled During the Deepwater Horizon Incident: Advanced Stages of Weathering. *Environ. Sci. Technol.* **2017**, *51*, 7412−7421.
(58) Wagner, S.; Ding, Y.; Jaffé, R. A new perspective on the apparent solubility of dissolved black carbon. *Front. Earth Sci.* **2017**, *5*, 75.
(59) Wagner, S.; Jaffé, R. Effect of photodegradation on molecular size distribution and quality of dissolved black carbon. *Org. Geochem.* **2015**, *86*, 1−4.
(60) Alan Roebuck, J.; Podgorski, D. C.; Wagner, S.; Jaffé, R. Photodissolution of charcoal and fire-impacted soil as a potential source of dissolved black carbon in aquatic environments. *Org. Geochem.* **2017**, *112*, 16−21.
(61) Wagner, S.; Jaffé, R.; Stubbins, A. Dissolved black carbon in aquatic ecosystems. *Limnol. Oceanogr. Lett.* **2018**, *3*, 168−185.
(62) Murphy, K. R.; Stedmon, C. A.; Wenig, P.; Bro, R. OpenFluor- an online spectral library of auto fluorescence by organic compounds in the environment. *Anal. Methods* **2014**, *6*, 658−661.
(63) Weishaar, J. L.; Aiken, G. R.; Bergamaschi, B. A.; Fram, M. S.; Fujii, R.; Mopper, K. Evaluation of specific ultraviolet absorbance as an indicator of the chemical composition and reactivity of dissolved organic carbon. *Environ. Sci. Technol.* **2003**, *37*, 4702−4708.
(64) Aeppli, C.; Carmichael, C. A.; Nelson, R. K.; Lemkau, K. L.; Graham, W. M.; Redmond, M. C.; Valentine, D. L.; Reddy, C. M. Oil weathering after the Deepwater Horizon disaster led to the formation of oxygenated residues. *Environ. Sci. Technol.* **2012**, *46*, 8799−8807.
(65) Kim, M.; Yim, U. H.; Hong, S. H.; Jung, J.-H.; Choi, H.-W.; An, J.; Won, J.; Shim, W. J. Hebei Spirit oil spill monitored on site by fluorometric detection of residual oil in coastal waters off Taean, Korea. *Mar. Pollut. Bull.* **2010**, *60*, 383−389.
(66) Lundstedt, S.; White, P. A.; Lemieux, C. L.; Lynes, K. D.; Lambert, I. B.; Öberg, L.; Haglund, P.; Tysklind, M. Sources, fate, and toxic hazards of oxygenated polycyclic aromatic hydrocarbons (PAHs) at PAH-contaminated sites. *Ambio* **2007**, *36*, 475−485.
(67) Podgorski, D. C.; Zito, P.; McGuire, J. T.; Martinovic-Weigelt, D.; Cozzarelli, I. M.; Bekins, B. A.; Spencer, R. G. M. Examining natural attenuation and acute toxicity of petroleum-derived dissolved organic matter with optical spectroscopy. *Environ. Sci. Technol.* **2018**, *52*, 6157−6166.
(68) Spencer, R. G. M.; Bolton, L.; Baker, A. Freeze/thaw and pH effects on freshwater dissolved organic matter fluorescence and absorbance properties from a number of UK locations. *Water Res.* **2007**, *41*, 2941−2950.
(69) Stedmon, C. A.; Bro, R. Characterizing dissolved organic matter fluorescence with parallel factor analysis: a tutorial. *Limnol. Oceanogr.: Methods* **2008**, *6*, 572−579.

https://doi.org/10.1021/acsestwater.1c00494
ACS EST Water 2022, 2, 994−1002